Revised version HE-D-11-02466, Hyceltec SI, Int. J. Hydrogen Energy, October 2011

Influence of support's oxygen functionalization on the activity of Pt/Carbon xerogels catalysts for methanol electro-oxidation

[1]C. Alegre, [1]M.E. Gálvez, [1]E. Baquedano, [2]E. Pastor, [1]R. Moliner, [1]M.J. Lázaro*

[1]Instituto de Carboquímica (CSIC), C/.Miguel Luesma Castán 4, 50018 Zaragoza, Spain

[2]Universidad de La Laguna, Dpto. Química-Física, Avda. Astrofísico Fco. Sánchez s/n, 38071 La Laguna (Tenerife), Spain

Abstract

Highly mesoporous carbon xerogels (CXs) were synthesized using two different resorcinol to catalyst, R/C, molar ratios and functionalized with different oxidation treatments. The synthesized carbon materials were used as supports for Pt particles, deposited by impregnation and reduction in formic acid. Both carbon supports and the catalysts prepared were characterized by means of N_2 physisorption, scanning and transmission electron microscopy, temperature programmed desorption and X-ray diffraction. The electrochemical activity of the catalysts towards the oxidation of carbon monoxide and methanol was assayed by means of cyclic voltammetry and chronoamperometry. Textural characterization of the materials prepared evidenced more developed and mesopore enriched porous structure for the carbon xerogel prepared using the highest R/C molar ratio. Enhanced textural properties of this material led to the preparation of highly active Pt-catalysts, which showed increased tolerance to CO and higher activity in methanol electro-oxidation, in comparison to Pt/E-TEK and the catalysts prepared in an analogous way using Vulcan XC-72R carbon black as support. Functionalization treatments resulted in enhanced dispersion, lower Pt crystal size and improved catalytic performance in the case of the catalysts prepared using the

* Corresponding author: Tel. +34 976 733 977; Fax: +34 976 733 318.
E-mail: mlazaro@icb.csic.es (M.J. Lázaro)

carbon xerogel possessing a less developed porous structure. Pt agglomeration was found to strongly determine the activity of the catalysts prepared. At high potentials, i.e. 1 V vs. RHE, the catalyst prepared using the carbon xerogel submitted to the most stringent oxidation treatment showed the highest specific peak activity towards methanol electro-oxidation, probably due to the positive influence of the presence of oxygen surface groups in Pt-carbon interaction, in spite of the higher agglomeration extent confirmed by TEM. On the other hand, at 0.60 V vs. RHE, highest activity towards methanol electro-oxidation was determined for the catalysts prepared using the non-functionalized carbon xerogel which can be explained in terms of enhanced reactant/product diffusion together with intrinsic higher catalytic activity due to lower Pt crystal size. In any case, the activity of this catalyst prepared using a carbon xerogel as support was found to be more than 2 times higher than the one determined for Pt/E-TEK, confirming the considerable improvement of the electro-catalytic system by means of optimization of the carbon support employed.

Keywords: carbon xerogel, functionalization, surface oxygen groups, Pt-catalysts, methanol electro-oxidation.

---

1. Introduction

Direct Methanol Fuel Cells (DMFCs) are regarded as promising candidates for power generation in practical applications ranging from portable power sources (for lap-tops, mobile phones, etc) to domestic and automotive electricity generation [1-3]. DMFCs make use of a liquid fuel, which can be easily stored and transported, making use of the already existing fuel distribution infrastructure. However their commercialization is still hindered by important technical challenges such as slow methanol oxidation kinetics in the anode [4,5]. To overcome this problem, research efforts are nowadays directed towards the obtaining of each time more active and resistant electrocatalysts, for cathode and anode [6], considering also partial or total substitution of Pt in these catalytic systems [7-10]. On the issue of improving electro-oxidation kinetics, present research focuses mainly on the development of high catalytic activity electrodes at low Pt content. One of the routes pursued is the development of new carbon supports of high electric conductivity, high surface area (high mesoporosity) and adjustable surface chemistry [11], such as carbon nanofibres [12], carbon nanotubes [13-15], carbon xerogels and aerogels [1,16-18], among others. Since their introduction by Pekala in 1989 [19], resorcinol–formaldehyde aqueous gels have been extensively studied. The reason why these materials have attracted an enormous attention is due to the possibility of fine-tuning their textural properties during the sol–gel method employed for their preparation. One may change the ratio of micro-, meso- and macropores and accordingly their specific surface areas over a wide range.

Surface chemistry has proven to be a key factor in carbon materials, leading to good performance when used as catalysts supports. Modification of surface chemistry can be achieved through different methods, and different surface functionalities containing heteroatoms such as O, N or S can be incorporated with different purposes.

Concretely, oxygen surface groups can be incorporated to carbon surface by means of different treatments, i.e. reaction with oxidizing gases such as ozone, oxygen, nitrous oxide, nitric oxide, carbon dioxide, etc., or oxidizing solutions, such as nitric acid, sodium hypochlorite, hydrogen peroxide, etc [20,21]. It has been generally acknowledged that the presence of a certain amount of surface oxygen groups can decrease the hydrophobicity of the carbon material, thus making its surface more accessible to the metal precursor during the impregnation with aqueous solution [22]. Moreover, the presence of such surface functionalities alters the pH values of aqueous carbon slurries and can thus have a considerable influence on the impregnation step of the catalyst preparation. Oxygen surface groups have been also frequently credited as nucleation sites for the generation of highly dispersed metallic crystallites [22]. For example, within the field of electrocatalysis, the effect of the support oxidation on the electrocatalytic features of CNF-supported Pt was studied by Guo et al. [23], Zaragoza-Martín et al. [24], Calvillo et al. [25] and Oh et al. [26]. They all found that pre-oxidation of the carbon support enhanced catalytic activity, depending on the type of CNF and oxidation treatment used. Figueiredo et al. [27] reported a remarkable increase in the activity of Pt and PtRu supported on multiwalled carbon nanotubes and high surface area mesoporous carbon xerogel submitted to oxidation pre-treatments.

In the present paper, mesoporous carbon xerogels were synthesized and functionalized by means of different oxidation treatments, in order to study the influence of the introduction of new surface oxygen groups, on the electrochemical performance of Pt-catalysts in the electro-oxidation of methanol.

2. Experimental

2.1. Carbon xerogels synthesis and functionalization

Resorcinol (1,3-dihydroxybenzoic acid)-formaldehyde organic gels were synthesized by the sol-gel method introduced by Pekala et al. [19]. Synthesis conditions employed in the present work are shown in Table 1, where R/F stands for molar ratio resorcinol to formaldehyde, R/C for molar ratios resorcinol to sodium carbonate (catalyst). Two different R/C molar ratios were employed, namely 50 and 800, in order to study the influence of this synthesis parameter on final carbon xerogels' textural properties. Reactants were mixed in the corresponding amounts and curing was carried out following the procedure described in detail elsewhere [16]. Finally, pyrolysis of the organic gels was performed in a tubular furnace at 800ºC for 3 hours under N_2 flow of 100 mL/min.

Carbon xerogels were then subjected to different oxidation treatments: Liquid phase oxidation treatments were performed at room temperature using 2 M HNO_3 for 30 min, and concentrated HNO_3 (65 %) for 120 min. Gas phase oxidation treatment consisted of flowing through a bed of 1g of each carbon material, 200 ml/min of a mixture of 5% O_2-N_2 for 3 hours at 450ºC. The oxidized carbon xerogels obtained were named as follows: Nd denotes treatment under diluted nitric acid, Nc corresponds to carbon xerogels treated in concentrated nitric acid, and O_2 denotes that the treatment was performed using the 5% O_2-N_2 gas mixture.

2.2. Catalysts preparation

Pt was deposited on the synthesized carbon xerogels and on Vulcan XC-72R carbon black by means of impregnation and reduction with formic acid. The amount of metallic precursor (H_2PtCl_6) was calculated to obtain a metal loading of 20% w/w. Each

carbon material was first dispersed in a 2M HCOOH solution at 80 ºC. Subsequently an aqueous solution of H_2PtCl_6 (Sigma-Aldrich) was added stepwise. Finally catalysts were filtered, thoroughly washed with ultrapure water, and dried overnight at 60ºC.

2.3. Physico-chemical and electrochemical characterization

The textural and morphological features of the different carbon supports and catalysts prepared were determined by means of nitrogen physisorption at -196ºC (Micromeritics ASAP 2020), scanning electron microscopy (SEM, Hitachi S-3400 N) and transmission electron microscopy (JEOL JEM-2000 FX II). Textural properties such as specific surface area, pore volume and pore size distribution were calculated from each corresponding nitrogen adsorption-desorption isotherms applying the Brunauer-Emmet-Teller (BET) equation, Barrett-Joyner-Halenda (BJH) and t-plot methods.

Surface chemistry of carbon supports was studied by temperature-programmed desorption. Such experiments were performed in a Micromeritics Pulse Chemisorb 2700 equipment, under a flow of helium with a heating rate of 10 °C min^{-1} from 150 ºC up to 1050 °C. The amounts of CO and CO_2 desorbed from the samples were analyzed by gas chromatography in a HP 5890 chromatograph with a thermal conductivity detector, packed columns Porapak N 10 ft and molecular sieve. These experiments give information about the surface oxygen groups created during the oxidation treatments. Acidic groups (carboxylic groups, lactones and anhydrides) are decomposed into CO_2 at low temperatures and basic and neutral groups (anhydrides, phenols and quinones) are decomposed into CO at high temperatures [28]. Gaussian function was used to fit each functional group contribution and the corresponding addition of Gaussian curves was fitted minimizing the square of the deviations by a numerical routine [29].

Inductively coupled plasma atomic emission spectroscopy (ICP-AES) was used to determine the amount of metal deposited. Catalysts were as well characterized by X-Ray Diffraction (XRD), using a Bruker AXS D8 Advance diffractometer, with a θ–θ configuration and using Cu-Kα radiation. Crystallite sizes were calculated from the Scherrer's equation on the (2 2 0) peak for platinum.

Electrochemical characterization has proven to be of key importance in determining the electrocatalytic activity of these materials [30,31]. Catalysts electrochemical activity towards the oxidation of carbon monoxide and methanol was studied by cyclic voltammetry and chronoamperometry at room temperature as in previous works [13,32].

A cell with a three-electrode assembly and an AUTOLAB potentiostat-galvanostat were used to carry out the electrochemical characterization. The counter electrode consisted on a pyrolitic graphite rod, while the reference electrode was a reversible hydrogen electrode (RHE). Therefore, all potentials in the text are referred to the latter. The working electrode consisted of a pyrolitic graphite disk (7 mm) with a thin layer of the electrocatalyst under study deposited onto it. For the preparation of this layer, an aqueous suspension consisting of 2 mg of Pt/C catalyst was obtained by ultrasonically dispersing it in Nafion solution 10%w/w (15 μL) and ultrapure water (500 μL) (Millipore). Subsequently an aliquot of 40 μL of the dispersed suspension was deposited on top of the graphite disk and dried under inert atmosphere prior its use.

After preparation, the electrode was immersed into deaerated 0.5 M H_2SO_4 electrolyte, prepared from high purity reagents (Merck) and ultrapure water (Milli-Q). The electrolyte was saturated with pure N_2 or CO (99.997%, Air Liquide), depending on the experiments.

Prior to the electrochemical characterization, the electrode was subjected to potential cycling between 0.05 and 1.10 V vs. RHE at a scan rate of 500 $mV \cdot s^{-1}$ until a stable voltammogram in the base electrolyte (0.5M H_2SO_4) was obtained. CO stripping voltammograms were obtained after bubbling this gas in the cell for 10 min at 0.20 V vs. RHE, followed by nitrogen purging to remove the excess of CO. The admission potential was selected considering that, for this value, maximum adsorbate coverage is achieved for CO adsorption on Pt. Afterwards, potential cycling between 0.05 V and 1.10 V vs. RHE at 20 $mV \cdot s^{-1}$ was carried out to follow CO oxidation. Electrochemical Pt active areas were determined from the integration of the current involved in the oxidation of a CO monolayer, taking into account that CO linearly adsorbs on Pt and assuming 420 $\mu C/cm^2$ involved in the oxidation process. Current values were normalized with respect to the electroactive area.

Cyclic voltammograms for the electrooxidation of methanol were carried out in a 2 M CH_3OH + 0.5 M H_2SO_4 solution, at scan rate of 20 $mV \cdot s^{-1}$, between 0.05 and 1.10 V vs. RHE. All the experiments were carried out at room temperature (25 ± 1 ºC), and current was normalized with respect to each catalyst metal amount (A/g Pt).

Chronoamperometries were performed at 0.60 V vs. RHE in a 2 M CH_3OH + 0.5 M H_2SO_4 solution, in order to evaluate the evolution of the electrocatalytic activity with time of the prepared catalysts in the electro-oxidation of methanol. All the experiments were carried out at room temperature (25 ± 1 ºC), and current was normalized with respect to each catalyst metal amount (A/g Pt).

3. Results and discussion

3.1. Textural characterization of the carbon supports

Table 2 shows the textural parameters determined by means of N_2 adsorption, for the synthesized carbon xerogels, CX_1 and CX_2, as well as for Vulcan carbon black. Carbon xerogels show high values of BET surface area, higher than the one determined for Vulcan carbon black. In fact, these materials possess an extensively developed porous structure, with an important contribution of micropores, but can be mainly considered as mesoporous carbons, with 89 and 85% of their pore volume corresponding to pores of diameter between 1.7 and 300 nm, and average pore sizes of 11.7 and 23.3, respectively. Average pore size is in fact the main difference that can be observed among CX_1 and CX_2, together with the considerably higher total pore and mesopore volume determined for CX_2, what is due to their different synthesis conditions.

The main role of the alkaline catalyst, Na_2CO_3, is to promote the de-protonation of the precursor, resorcinol, initiating the addition reaction that leads to the formation of the hydroxymethyl derivates, which are essential for the following condensation reaction. Due to higher gelation rates in the presence of excess catalyst, it is generally believed that low R/C molar ratios result in small polymer particles (about 3-5 nm size) which are highly interconnected by large necks giving the gel a fibrous appearance. In contrast, high R/C molar ratios result in the formation of large particles (16 to 200 nm in diameter) which are connected by narrow necks in a “string-of-pearls” fashion [33,34]. Drying under conventional evaporation conditions cause a more drastic shrinkage of the porous structure of the gel, vis-à-vis other drying procedures such as supercritical drying. However, Saliger and co-workers [35] observed that carbon gels prepared using

high R/C ratios presented enough mechanical strength to withstand the capillary pressured generated during subcritical drying, leading to minimal collapse of their porous structure. This fact explains the more developed porous structure of CX_2 in comparison to CX_1, as a consequence of the higher R/C ratio employed in the synthesis of the former.

In general, for carbon xerogels CX_1 and CX_2 subjected to liquid phase oxidation with nitric acid, a slight decrease in BET surface area was observed, especially when using concentrated nitric acid. This change in the porous structure of these carbon materials is due to partial collapse of their porous structures, particularly in the case of the more intensive oxidation treatment using concentrated nitric acid. In contrast, oxidation in the presence of $5\%O_2$-N_2 leads to higher S_{BET} values in all cases. Gas-phase oxidation results in relative pore enlargement by means of partial gasification of the carbon material, particularly affecting microporosity. Depending on the initial pore structure of the carbon material, micropores are enlarged to the size of mesopores, i.e. see higher mesopore volumes determined for CX_1_O_2 and CX_2_O_2, together with the opening up of some narrow micropores accessible to oxygen, leading to the formation of medium size micropores, contributing to a slight increase of both total and micropore volume, i.e. in the case of CX_2-O_2. Minor changes in average pore size can be assigned to preferable pore enlargement towards the formation of new pores of relatively lower size than the ones prevailing in the untreated carbon xerogels, i.e. lower size mesopores at the expense of micropores.

3.2. Oxygen functionalization of the carbon supports

Figure 1 shows the amounts of CO and CO_2 evolved during temperature programmed desorption (TPD) for CX_1 and CX_2, before and after the different oxidation treatments. The total amounts of oxygen are presented in Table 3, calculated

from TPD data. Untreated samples contain an amount of oxygen between 1.7–1.9 wt.%. The largest creation of oxygen groups was obtained for the carbon materials submitted to concentrated nitric acid functionalization, with an oxygen content between 9.8-10.3 wt.%. Treatment in the presence of diluted nitric acid resulted in a milder surface oxidation (oxygen content between 2.1-4.3 wt.%), whereas in the presence of 5%O_2-N_2, an intermediate degree of functionalization (oxygen content between 4.7-5.9 wt.%), between the results obtained using concentrated and diluted nitric acid can be observed.

Deconvolution of the TPD, Table 3, shows that functionalization with nitric acid results in a increase in the concentration of carboxylic surface groups. Moreover, for both CX_1 and CX_2, the amount of phenolic and carbonyl/quinone surface groups notably increases after functionalization, and in less extent lactones. Phenolic and carbonyl/quinone surface groups have been established to be responsible for the strong adsorption of Pt on carbon [22]. It must be noted here that Vulcan carbon black was submitted as well to identical oxidation treatments. Carbon black oxidation has been reported as a perspective way of improving their performance as catalyst supports [36]. However, probably due to its inertness and stability, this material was found to be practically reluctant to the oxidation treatments considered within this work. Vulcan carbon black itself shows initially a very poor surface chemistry, with an oxygen content of 0.6 wt. %. Even under the most intensive of the oxidation conditions employed, i.e. liquid phase oxidation in the presence of concentrated nitric acid, oxygen content in the treated carbon black only amounts to 2.3 wt. %., about 5 times lower than in the case of any of the carbon xerogels synthesized submitted to identical oxidation treatments.

3.3. Characterization of the Pt-catalysts

Table 4 shows the textural parameters determined by means of N_2 adsorption, for the catalysts prepared using the carbon xerogels, CX_1 and CX_2, and Vulcan carbon black. Surface area and mesopore volume decrease in all cases after the incorporation of the active phase. The partial loss of mesopore volume as a consequence of Pt loading results as well in the slight increase of micropore volume that can be observed in most cases. However, in spite of this partial blockage of the porous structure, the catalysts, concretely those prepared using the synthesized carbon xerogels and moreover those prepared using CX_2, maintain their enhanced textural features, with abundant mesopores and acceptable values of surface area, higher in all cases than the one determined for the catalyst prepared using Vulcan carbon black.

With respect to Pt crystal sizes deduced from the XRD patterns acquired for the different catalysts, shown in Table 5 and Figure 2, respectively, they range from 2.4 to 5.7 nm. Except for the xerogels treated with concentrated nitric acid, lower Pt crystal sizes were measured for the catalysts prepared using the carbon xerogel CX_2 than when using CX_1, probably due to its more developed porous structure, favouring metal dispersion. Catalyst prepared using Vulcan carbon black as support shows a Pt crystal size of 3.4 nm, lower in any case than the one calculated for the rest of the catalysts prepared using the non-oxidized and oxidized carbon xerogels, with the exception of the catalyst prepared using the carbon xergoel CX_2 submitted to gas phase oxidation, $Pt/CX_2\text{-}O_2$, showing a crystal size of 2.4 nm.

Regarding the effect of the functionalization treatment on crystal size, it can be observed that for the carbon xerogel with a less developed structure, CX_1, functionalization favours metal dispersion (except for the functionalization with concentrated nitric acid), decreasing Pt crystal size; whereas for CX_2, possessing a more developed porous structure, functionalization does not contribute positively, and Pt

crystal sizes even increase when supports are submitted to oxidation treatments. In fact, in this case only oxidation with oxygen leads to a slightly lower Pt crystal size. The increased concentration, and thus proximity, of oxygen sites for Pt anchoring may result in the deposition and crystal growth of Pt in the form of crystallites of increased size, in comparison to the non-fucntionalized support.

TEM micrograms evidenced in general favoured dispersion when employing the functionalized carbon supports, especially in the case of pre-treated CX_2, which possesses a more developed porous structure. Figure 3a and 3b show two TEM images acquired for the catalysts prepared using non-oxidized carbon xerogel CX_2, Pt/CX_2, and Figure 3c an image corresponding to the catalyst prepared using the same carbon material after oxidation in the presence of diluted nitric acid, Pt/CX_2-Nd. Though Pt crystal size derived from XRD difractograms was lower for Pt/CX_2 than for Pt/CX_2-Nd, 3.6 vs. 4.1 nm, particles appear well dispersed in some areas, see Figure 3b, it can be observed how the dispersion of Pt particles notably improves after functionalization of the carbon material using diluted nitric acid. Metallic particles on the catalyst prepared using the non-functionalized carbon xerogel tend to agglomerate in some sections of the catalyst explored, see Figure 3a, whereas they appear more properly dispersed on the surface of the diluted nitric acid treated material, see Figure 3c, though the presence of some agglomerates was also detected. The creation of surface functionalities, most probably those which are thermally more stable, such as phenols, act as anchoring sites for Pt particles, resulting in an enhanced dispersion of the active phase [22]. Figure 3d shows a TEM micrograph obtained for the catalyst prepared using the carbon xerogel submitted to oxidation in the presence of concentrated nitric acid, Pt/CX_2-Nc. Dispersion of the active phase over the surface of the carbon material seems to be also favoured in this case, however, too intensive functionalization results in particle

agglomeration and thus, increased Pt crystal size, in total agreement with the results of XRD characterization. Figure 3d shows a TEM micrograph obtained for the catalyst prepared using the carbon xerogel submitted to gas phase oxidation in the presence of 5%O_2-N_2, Pt/CX_2-O_2. Gas phase functionalization of the support enhances as well Pt particle dispersion on the carbon surface. TEM image acquired for the catalyst prepared using Vulcan carbon black as support is shown in Figure 3e. As can be observed, good dispersion of the active phase can be as well achieved when using this carbon material as support. In spite of its less developed porous structure and the lack of oxygen functionalities on its surface, Pt particles appear adequately distributed. The different morphology of this material can be also observed in this image, its structure mostly composed by spherical primary particles which internally present a certain degree of graphitical short-range order [37]. This sort of ordered structure results, in fact, in an enhanced ability of this carbon material to disperse the electronic charge of the loaded metal, which may explain the good distribution of Pt particles achieved in spite of other structural drawbacks in comparison to the synthesized carbon xerogels.

3.4. Electrochemical characterization and catalytic activity

Pt catalysts supported on carbon xerogels were characterized by cyclic voltammetry (CV). CO stripping was performed in order to establish the influence of the functionalization of the support in the electrochemical performance of each of the catalysts towards CO electro-oxidation. CO-stripping voltammograms obtained are shown in Figure 4. The second cycles recorded after CO-stripping, which correspond to the voltammograms in the base electrolyte for clean surfaces, are also shown. This scan is carried out in order to check that the oxidation of CO has been completed.

Figure 4a, 4b, 4c and 4d show the voltammograms for CO oxidation in the presence of the catalyst prepared using the carbon xerogels as supports, before and after

functionalization. Onset potentials for CO oxidation are in general lower for carbon xerogels than in the case of the commercial and the Vulcan-supported catalyst (shown in Figure 4e), 0.58 V vs. RHE for Pt/CX_1 and 0.62 V vs. RHE for Pt/CX_2 vs 0.65 V vs. RHE for Pt/CB-Vulcan and 0.70 V vs. RHE for Pt-E-TEK. It is also noticeable that in general, onset potentials for Pt/CX_1 catalysts are more negative than for Pt/CX_2 catalysts. Regarding the effect of functionalization, must be noted as well that onset CO oxidation potentials for functionalized Pt/CX catalysts, are all the time lower than the ones shown by the catalysts prepared using the non-functionalized carbon support, especially when using CX_1 and CX_2 treated with diluted nitric acid, i.e. 0.42 V vs. RHE and 0.56 V vs. RHE, respectively.

It can also be observed that in the case of Pt/CX_1, CO oxidation presents two peaks. This fact becomes evident also at the sight of Figures 4b, 4c and 4d, which correspond to the catalysts prepared using the oxidized carbon xerogels as support, also in the case of CX_2. These voltammograms generally present a first peak of CO oxidation centred at about 0.70 V vs. RHE, followed by a second one centred at approximately 0.80 V vs. RHE. The intensity of the first peak is all the time higher for the catalysts prepared using CX_1 as the starting material, whereas for the catalyst prepared using CX_2 is the second contribution which becomes more important. Maillard and co-workers [38] studied the behaviour in CO-electrooxidation of carbon black-supported catalysts which showed different degrees of metal particle agglomeration. They observed that in fact CO monolayer oxidation was strongly influenced by Pt particle size, and that the catalytic activity of particles with diameter above 3 nm approached that of polycrystalline behaviour, differing from the one observed for Pt sizes lower than 3 nm. They reported however remarkable activity for Pt agglomerates in comparison to isolated Pt particles or polycrystalline Pt, catalysing CO oxidation at

considerably lower overpotentials. In fact, they observed the same double-peak CO oxidation voltammograms for those catalysts comprising Pt agglomerates along with isolated single crystalline Pt nanoparticles from 2 to 6 nm size, and assigned the more negative to CO oxidation on Pt agglomerates and the more positive to CO oxidation over the isolated nanoparticles. Furthermore, they ascribed enhanced catalytic activity of Pt agglomerates to high concentration surface defects. The observations of Maillard et al. are consistent with our observations: in general, catalysts showing Pt crystal sizes higher than 3.8 nm clearly show this double-peak shaped voltammogram. Indeed, with respect to the influence of support's functionalization, in the case of CX_1 the intensity of the first peak decreases for the catalysts prepared using the functionalized supports, pointing to a less important presence and activity of Pt agglomerates due to enhanced dispersion. However, in agreement with what was observed after their physico-chemical characterization, metal dispersion is favoured when using CX_2 as support, due to its more developed porous structure. Voltammogram for Pt/CX_2 barely show the first peak of CO oxidation and in the case of CX_2-supported catalysts, functionalization using diluted nitric acid results in a sharp shaped peak centred at 0.78 V vs. RHE whereas the first peak at 0.68 V vs. RHE becomes almost a shoulder of the following one, pointing to predominance of dispersed Pt nanoparticles over agglomerates. These observations are in total agreement with the results obtained by means of TEM analyses of the CX_2 supported catalysts, see Figure 3.

Methanol electro-oxidation voltammograms are shown in Figure 5. Note that activity is shown as mass activity in these plots, i.e. current density as a function of Pt content in each catalyst. Figures 5a, 5b, 5c and 5d show the methanol electro-oxidation voltammograms obtained for the catalysts prepared using the synthesized carbon xerogels. In all cases, the catalysts prepared using CX_2 as support, either before or after

functionalization, show higher peak current densities than CX_1-supported ones. Functionalization slightly improves the behaviour of these CX_1-supported catalysts, especially when using diluted nitric acid, as can be seen in Figure 5b. However, the positive influence of the functionalization of the carbon support is substantially more noticeable when using CX_2. Less developed porous structure of CX_1, which as well influences reactant and product diffusion to and out of Pt actives sites, together with the higher Pt crystal sizes and Pt agglomeration observed for this series of catalyst, may account for the lower activity of these catalysts in comparison to CX_2-supported ones. The highest peak current densities were registered for the catalysts prepared using CX_2 oxidized with both concentrated nitric acid and oxygen, Pt/CX_2-Nc and Pt/CX_2-O_2. In the case of the Pt/CX_2-Nc, its electrochemical surface area (ECSA), derived from the integration of the oxidation peaks in the CO stripping voltammogram, amounts to 27 m^2/g Pt, whereas a value of 39 m^2/g Pt was measured for the catalyst prepared using the non-fucntionalized support, Pt/CX_2. This decrease in ECSA can be ascribed to Pt agglomeration and higher particle size, confirmed by means of XRD and TEM. In spite of this fact, the oxygen surface groups introduced upon functionalization of the carbon support favour the electrocatalytic activity of the deposited Pt. Note than increased oxygen content in the support corresponds to higher specific peak current densities in terms of A/m^2 Pt, i.e. approximately 20 A/m^2 Pt in the case of Pt/CX_2-Nc, 15 A/m^2 Pt for Pt/CX_2-O_2, and 11 and 6 A/m^2 Pt for Pt/CX_2-Nd and Pt/CX_2, respectively. In this sense, oxygen functionalities on the support may favour electronic transfer from the metallic particles to the bulk of the carbon material, enhancing the electrocatalytic performance.

Figure 5e shows the voltammograms obtained for both the commercial E-TEK catalysts and the one prepared using Vulcan carbon black as support. Commercial E-

TEK catalyst shows slightly higher activity, in terms of both onset potential and peak current density, than the catalysts prepared in this work using Vulcan carbon black, what can be ascribed to lower Pt crystal size in the case of E-TEK catalyst.

The results of chronoamperometric curves towards methanol oxidation are shown in Figure 6a. Catalysts prepared using non-functionalized and functionalized CX_1 as support present the lower activity of this series of catalyst in comparison to the one prepared using Vulcan carbon black and the commercial E-TEK catalyst. In fact, E-TEK catalyst shows the highest current density, followed by the Vulcan-supported catalyst. Note that chronoamperometric measurements were performed for a maximal of 15 minutes. Catalysts stability and the evaluation of their activity over prolonged periods of time will be subject of future studies.

As observed in Figure 5, both CX_2 functionalization using concentrated nitric acid and gas phase oxidation using 5%O_2-N_2 result in a sharp increase of the peak current densities measured during methanol electro-oxidation, however, onset potentials are much lower for the catalyst prepared using non-oxidized CX_2. Functionalization thus influenced peak current densities but not the potential at which methanol electro-oxidation sets off. As a result of this, and taking into account that this experiments were performed at 0.60 V vs. RHE, chronoamperometric curves for methanol oxidation shown in Figure 6b evidence higher current densities for the catalyst prepared using the non-functionalized CX_2 as support, in comparison to the rest of the catalyst prepared using the oxidized carbon material, Vulcan carbon black and the commercial E-TEK catalyst. Physico-chemical characterization showed lower Pt crystal sizes for Pt/CX_2 than for the catalyst prepared using the differently oxidized CX_2s, though more adequate distribution of the metallic particles was observed by TEM. Thus, in spite of the positive influence of functionalization, which improves active phase dispersion and

probably also its interaction with the carbon support, the somehow predominant presence of Pt crystallites of lower size, co-existing with Pt agglomerates in Pt/CX_2, may result in a higher activity towards methanol electro-oxidation vis-à-vis the rest of catalysts prepared using the functionalized supports. Moreover at 0.60 V vs. RHE, higher intrinsic catalytic activity due to the presence of this lower size Pt crystals may control the process of methanol electro-oxidation, whereas at more positive operation potentials, enhanced diffusion due to the more developed porous structure of this material makes the rest of the catalytic sites accessible and able to contribute to the overall reaction, in spite of their particular crystal size and distribution.

4. Conclusions

Two carbon xerogels were synthesized and functionalized through different oxidation treatments, with the aim of optimizing its textural properties and surface chemistry by means of the introduction of oxygen surface groups.

These carbon xerogels were used as supports in the preparation of several Pt-catalysts which were characterized and tested for CO and methanol electro-oxidation via cyclic voltammetry and chronoamperometry.

Catalyst physico-chemical characterization evidenced more developed porous structures for the two synthesized carbon xerogels in comparison to Vulcan XC-72R carbon black, which was also included in this study for the sake of comparison. The carbon xerogel prepared using the highest R/C ratio (800), CX_2, showed an even more developed porous structure, with an important contribution of mesopores. Catalyst textural characterization evidenced certain extent of pore blockage, with Pt depositing mainly on mesopores, though both carbon materials maintained their enhanced porous structures. Crystal sizes calculated by means of X-Ray Diffraction were lower in the case of the catalyst prepared using carbon xerogel CX_2. Functionalization resulted in

smaller Pt crystal sizes in the case of CX_1, however, the introduction of surface functionalities on the surface of the carbon xerogel possessing the more developed porous structure, CX_2, resulted in general in higher crystal sizes. TEM clearly evidenced favoured dispersion of the active phase upon functionalization, though even the catalyst prepared using the non-functionalized carbon xerogel CX_2 presented areas were Pt was well dispersed, matching the lower crystal size calculated from the XRD difractograms.

The catalysts prepared using the synthesised carbon xerogels showed increased CO tolerance, being able to oxidize CO at more negative potentials, in comparison to Pt/CB-Vulcan catalyst and commercial Pt-E-TEK catalyst. Voltammogramns presented in some cases a double-peak shape which has been assigned to the simultaneous presence of both well dispersed nanosized Pt (more positive peak) and Pt agglomerates (more negative peak). Functionalization resulted in a decrease of the intensity of the more negative peak, pointing to an increased presence of well dispersed Pt particles. Methanol electro-oxidation was found to be more sensitive towards particle size, concretely in terms of the onset potentials derived from the corresponding voltammograms. More agglomerated Pt in the catalyst prepared using the carbon xerogel CX_1 resulted in a hindered activity towards methanol oxidation, in spite of any of the functionalization treatments employed and the more developed porous structure characterising this material, in comparison to E-TEK commercial catalyst and the analogous catalyst prepared using Vulcan carbon black as support. Though at more positive potentials the catalyst prepared using the functionalized supports evidenced higher current densities in the voltamperometric runs, the catalyst prepared using non-functionalized carbon xerogel CX_2 yielded the highest activity towards methanol oxidation in terms of onset potential, and as a consequence showed increased activity during the chronoamperometric experiments performed at 0.60 V vs. RHE, with respect

to the rest of the catalyst prepared using the rest of the synthesized carbon materials, Vulcan carbon black and the commercial E-TEK catalyst. Its enhanced activity can be due to the presence of highly dispersed nanosized Pt, in spite of the presence of active phase agglomerates, and the mesopore-enriched well developed porous structure of the carbon xerogel used as support.

Acknowledgements

Authors want to acknowledge FEDER and the Spanish MICINN for financial support under the projects MAT2008-06631-C03-01 and MAT2008-06631-C03-02. M.E. Gálvez is indebted to the Spanish Ministry of Science and Innovation (MICINN) for her Juan de la Cierva post-doctoral fellowship.

References

[1] Arbizzani C., Beninati S., Manferrari E., Soavi F., Mastragostino M.. Cryo- and xerogel carbon supported PtRu for DMFC anodes. J. Power Sources 2007; 172: 578-86.

[2] Kamarudina S.K, Achmad F., Daud W.R.W. Overview on the application of direct methanol fuel cell (DMFC) for portable electronic devices. Int. J. Hydrogen Energy 2009; 34: 6902-16.

[3] García M.F., Sieben J.M., Pilla A.S., Duarte M.M.E., Mayer C.E. Int. J. Hydrogen Energy 2008; 33: 3517 –3521.

[4] Aricò A.S., Baglio V., Antonucci V. Direct Methanol Fuel Cells. Nova Publishers. ISBN: 978-1-61122-447-4.

[5] Basri S., Kamarudin S.K., Daud W.R.W., Yaakub Z. Int. J. Hydrogen Energy 2010; 35: 7957-7970.

[6] Fang B., Wanjala B.N., Yin J., Loukrakpam R., Luo J., Hu X., Last J., Zhong C.J.. Electrocatalytic performance of Pt-based trimetallic alloy nanoparticle catalysts in proton exchange membrane fuel cells. . Int. J. Hydrogen Energy2011; In press, DOI: 10.1016/j.ijhydene.2011.05.066.

[7] Moreira J., del Angel P., Ocampo A.L., Sebastián P.J., Montoya J.A., Castellanos R.H. Int. J. Hydrogen Energy 2004; 29: 915 – 920.

[8] Kim J.Y., Oh T.-K., Shin Y., Bonnett J., Weil K.S. Int. J. Hydrogen Energy 2011; 36: 4557-4564.

[9] Alcaide F., Álvarez G., Cabot P.L., Grande H.-J., Miguel O., Querejeta A. Int. J. Hydrogen Energy 2011; 36: 4432-4439.

[10] Grigoriev S.A., Lyutikova E.K., Martemianov S., Fateev V.N. Int. J. Hydrogen

Energy 2007; 32: 4438-4442.

[11] Zainoodin A.M., Kamarudin S.K., Daud W.R.W. Electrode in direct methanol fuel cells. Int. J. Hydrogen Energy 2010; 35: 4606-21.

[12] Sebastián D., Calderón J.C., González-Expósito J.A., Pastor E., Martínez-Huerta M.V., Suelves I., Moliner R., Lázaro M.J. Influence of carbon nanofiber properties as electrocatalyst support on the electrochemical performance for PEM fuel cells. Int. J. Hydrogen Ene 2010; 35: 9934-94.

[13] Cui Z., Liu C., Liao J., Xing W. Highly active PtRu catalysts supported on carbon nanotubes prepared by modified impregnation method for methanol electro-oxidation. Electrochim.Acta 2008; 53: 7807-11.

[14] Liu X., Villacorta R., Adame A., Kannan A.M. Int. J. Hydrogen Energy 2011; 36: 10877-10883.

[15] Esmaeilifar A., Yazdanpour M., Rowshanzamir S., Eikani M.H. Int. J. Hydrogen Energy 2011; 36 : 5500-5511.

[16] Job N., Ribeiro M.F., Lambert S., Colomer J.F., Marien J., Figueiredo J.L., Pirard J.P.. Highly dispersed platinum catalysts prepared by impregnation of texture-tailored carbon xerogels. J. Catal 2006; 240: 160-71.

[17] Kim H.J., Kim W.I., Park T.J., Park H.S., Suh D.J.. Highly dispersed platinum–carbon aerogel catalyst for polymer electrolyte membrane fuel cells. Carbon 2008; 46: 1393-1400.

[18] Smirnova A., Dong X., Hara H., Vasiliev A., Sammes N.. Novel carbon aerogel-supported catalysts for PEM fuel cell application. Int. J. Hydrogen Energy 2005; 30: 149–58.

[19] Pekala R.W. Organic aerogels from the polycondensation of resorcinol with formaldehyde. J Mater Sci 1989; 24: 3221-27.

[20] Park S.J., Park J.M., Seo M.K. Electrocatalytic properties of graphite nanofibers-supported platinum catalysts for direct methanol fuel cells. J. Colloid Interface Science 2009; 337: 300-303.

[21] Barton S. S., Evans M. J. B., Halliop E., MacDonald J. A. F. Acidic and basic sites on the surface of porous carbon. Carbon 1997; 35: 1361-66.

[22] Fraga M. A., Jordão E., Freitas M. M. A., Faria J. L., Figueiredo J. L. Properties of Carbon-Supported Platinum Catalysts: Role of Carbon Surface Sites. J. Catal. 2002*;* 209: 355–364,.

[23] Guo J., Sun G., Wang Q., Wang G., Zhou Z., Tang S., Jiang L., Zhou B., Xin Q. Carbon nanofibers supported Pt-Ru electrocatalysts for direct methanol fuel cells. Carbon 2006; 44: 152-57.

[24] Zaragoza-Martín F., Sopeña-Escario D., Morallón E., Salinas-Martínez de Lecea C. Pt/carbon nanofibers electrocatalysts for fuel cells. Effect of the support oxidizing treatment. J. Power Sources 2007; 171: 302-9.

[25] Calvillo L., Gangeri M., Perathoner S., Centi G., Moliner R., Lázaro M.J. Effect of the support properties on the preparation and performance of platinum catalysts supported on carbon nanofibers. J. Power Sources 2009; 192: 144-50.

[26] Oh H.S., Kim K., Ko Y.J., Kim H. Effect of chemical oxidation of CNFs on the electrochemical carbon corrosion in polymer electrolyte membrane fuel cells. Int. J. Hyd. Energy 2010; 35: 701-8.

[27] Figueiredo J.L., Pereira M.F.R, Serp P., Kalck P., Samant P.V., Fernandes J.B, Development of carbon nanotube and carbon xerogel supported catalysts for the electro-oxidation of methanol in fuel cells. Carbon 2006; 44: 2516-22.

[28] Figueiredo J. L., Pereira M. F. R., Freitas M. M. A., Órfão J. J. M. Modification of the surface chemistry of activated carbons. Carbon 1999; 37: 1379-1389.

[29] Sebastián D., Suelves I., Moliner R., Lázaro M.J. The effect of the functionalization of carbon nanofibers on their electronic conductivity. Carbon 2010; 48: 4421-31.

[30] Srinivasan. Fuel Cells: From fundamentals to applications. Springer. ISBN: 0-387-25116-2 (2006).

[31] Bagotzky V.S., Vassiliev Yu. B.. Mechanism of electro-oxidation of methanol on the platinum electrode. Electrochim. Acta 1967; 12: 1323-1343.

[32] Alegre C., Calvillo L., Moliner R., González-Expósito J.A., Guillén-Villafuerte O., Martínez Huerta M.V., Pastor E., Lázaro M.J.. Pt and PtRu electrocatalysts supported on carbon xerogels for direct methanol fuel cells. J. Power Sources 2011; 196: 4226-4235.

[33] Saliger R., Bock V., Petricevic R., Tillotson T., Geis, S., Fricke J. Carbon aerogels from dilute catalysis of resorcinol with formaldehyde. J. Non-Cryst. Solids 1997; 221: 144-50.

[34] Al-Muhtasheb S.A., Ritter J.A. Preparation and properties of resorcinol-formaldehyde organic and carbon gels. Adv. Mater. 2003; 15: 101-14.

[35] Saliger R., Fischer U., Herta C., Fricke J. High surface area carbon aerogels for supercapacitors. J. Non-Cryst. Solids 1998; 225: 81-5.

[36] Antolini E. Carbon supports for low-temperature fuel cell catalysts. Appl. Catal. B: Environ. 2009; 88: 1-24.

[37] Calvillo L., Celorrio V., Moliner R., Lázaro M.J.. Influence of the support on the physicochemical properties of Pt electrocatalysts: Comparison of catalysts supported on different carbon materials. Mater. Chem. Phys 2011; 127: 335-41.

[38] Maillard F., Schreier S., Savinova E.R., Weinkauf S., Stimming U. Influence of particle agglomeration on the catalytic activity of carbon-supported Pt

nanoparticles in CO monolayer oxidation. Phys. Chem. Chem. Phys 2005; 7: 385-93.

Table 1. Carbon xerogel synthesis parameters.

Carbon xerogel	R/F	R/C	pH
CX_1	0.5	50	6.0
CX_2		800	

Table 2. Surface area, total, micropore and mesopore volumes, and average pore size for the synthesised carbon xerogels.

Carbon support	**S_{BET}** (m^2/g)	**V_{pore}** (cm^3/g)	**V_{micro}** (cm^3/g)	**V_{meso}** (cm^3/g)	**Average pore size** (nm)
CX_1	534	1.07	0.11	0.96	11.7
CX_2	528	1.79	0.15	1.64	23.3
Vulcan	224	0.47	0.01	0.46	11.0
CX_1-Nd	517	1.04	0.17	0.87	13.0
CX_1-Nc	497	0.88	0.06	0.82	9.0
CX_1-O_2	702	1.07	0.08	0.99	8.2
CX_2-Nd	506	1.75	0.11	1.64	23.4
CX_2-Nc	441	1.79	0.14	1.65	23.0
CX_2-O_2	604	1.82	0.16	1.66	22.3

Table 3. Deconvolution of the CO and CO_2 TPD profiles for the carbon supports before and after functionalization.

	Oxygen content (% wt.)	*Cbx*	*Anh*	*Lac*	*Ph*	*Cbn/Qn*
CX_1	1.9	0.30	0.01	0.11	0.00	0.33
CX_1-Nd	4.3	0.39	0.09	0.24	0.17	0.64
CX_1-Nc	9.8	0.77	0.30	0.35	1.95	1.05
CX_1-O_2	4.7	0.06	0.00	0.56	0.91	0.80
CX_2	1.7	0.15	0.02	0.07	0.33	0.24
CX_2-Nd	2.1	0.14	0.02	0.08	0.37	0.44
CX_2-Nc	10.3	0.16	0.49	0.35	2.67	1.29
CX_2-O_2	5.9	0.11	0.02	0.50	1.66	0.69

Cbx: *Carboxylic;* ***Anh:*** *Anhydride;* ***Lac:*** *Lactone****;*** ***Ph:*** *Phenolic*
Cbn/Qn: *Carbonyl/Quinone, in mmol/g.*

Table 4. Surface area, total, micropore and mesopore volumes, and average pore size for the synthesised catalysts.

Carbon support	**S_{BET}** (m^2/g)	**V_{pore}** (cm^3/g)	**V_{micro}** (cm^3/g)	**V_{meso}** (cm^3/g)	**Average pore size** (nm)
Pt/CX_1	472	0.84	0.13	0.71	10.0
Pt/CX_1-Nd	467	0.95	0.15	0.80	12.7
Pt/CX_1-Nc	428	0.76	0.11	0.65	10.1
Pt/CX_1-O_2	594	1.05	0.20	0.85	11.6
Pt/CX_2	380	1.08	0.14	0.94	23.5
Pt/CX_2-Nd	349	1.27	0.11	1.16	25.5
Pt/CX_2-Nc	391	1.33	0.14	1.19	24.9
Pt/CX_2-O_2	465	1.34	0.17	1.17	22.1
Pt-E-TEK	171	0.35	0.05	0.30	12.3
Pt/CB-Vulcan	173	0.38	0.03	0.35	11.9

Table 5. Crystal size (XRD) and Pt amount, measured for both the synthesised and commercial catalysts.

Catalyst	***Crystal size (nm)***	***% wt. Metal deposited***
Pt/CX_1	5.3	16.9
Pt/CX_1-Nd	4.6	15.1
Pt/CX_1-Nc	5.3	19.7
Pt/CX_1-O_2	4.4	7.9
Pt/CX_2	3.6	17.9
Pt/CX_2-Nd	4.1	19.5
Pt/CX_2-Nc	5.7	21.9
Pt/CX_2-O_2	2.4	17.6
Pt-E-TEK	3.0	17.0
Pt/CB-Vulcan	3.4	16.7

Figure captions

Figure 1. mmol/g of surface oxygen groups desorbed as CO or CO_2 in TPD experiments.

Figure 2. Diffractograms obtained by XRD for: a) Pt/CX_1-catalysts b) Pt/CX_2-catalysts

Figure 3. TEM micrographs for the electrocatalysts: a) Pt/CX_2 (Section 1); b) Pt/CX_2 (Section 2); c) Pt/CX_2-Nd; and d) Pt/ CX_2-Nc e) Pt/CX_2-O_2; and f) Pt/CB-Vulcan.

Figure 4. Cyclic voltammograms during CO stripping in a 0.5 M H_2SO_4 solution. Scan rate ν = 0.02 V/s.

Figure 5. Cyclic voltammograms for the electrooxidation of methanol in a 2 M CH_3OH + 0.5 M H_2SO_4 solution. Scan rate v = 0.02 V/s.

Figure 6. Current density–time curves recorded in a 2 M CH_3OH + 0.5 M H_2SO_4 solution at E = 0.60 V vs. RHE, in the presence of a) CX_1 supported catalyst and b) CX_2 supported catalysts, in comparison to the commercial and Vulcan supported catalysts. The upper part of the graph in Figure 6 a shows a detailed plot for CX_1-supported catalysts.

Figure 1

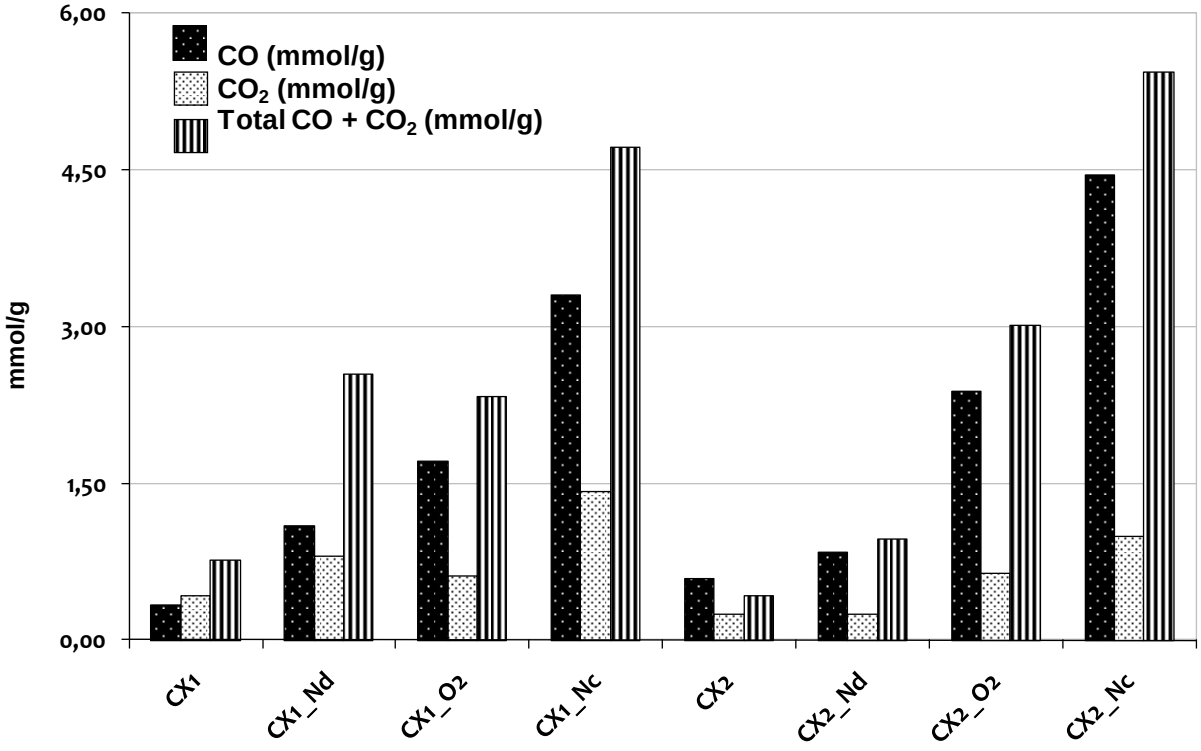
6,00
4,50
3,00
1,50
0,00
mmol/g
CO (mmol/g)
CO2 (mmol/g)
Total CO + CO2 (mmol/g)
CX1
CX1_Nd
CX1_O2
CX1_Nc
CX2
CX2_Nd
CX2_O2
CX2_Nc

Figure 2.

a)

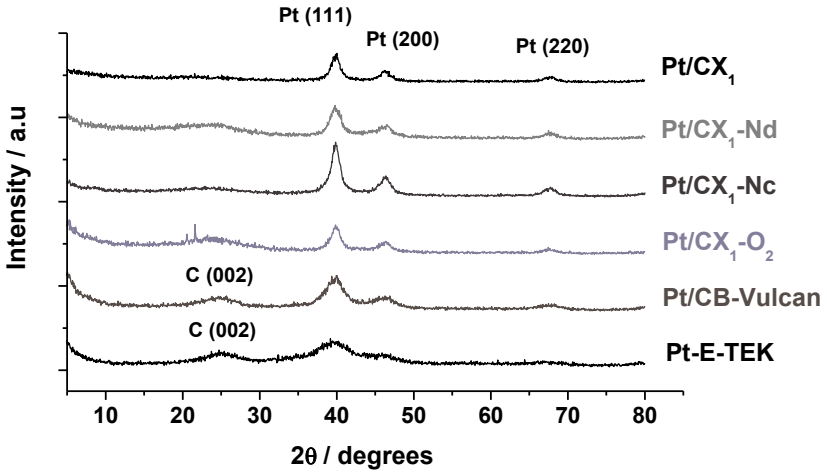
Pt (111)
Pt (200)
Pt (220)
Pt/CX1
Pt/CX1-Nd
Pt/CX1-Nc
Pt/CX1-O2
C (002)
Pt/CB-Vulcan
C (002)
Pt-E-TEK
Intensity / a.u
10
20
30
40
50
60
70
80
2θ / degrees

b)

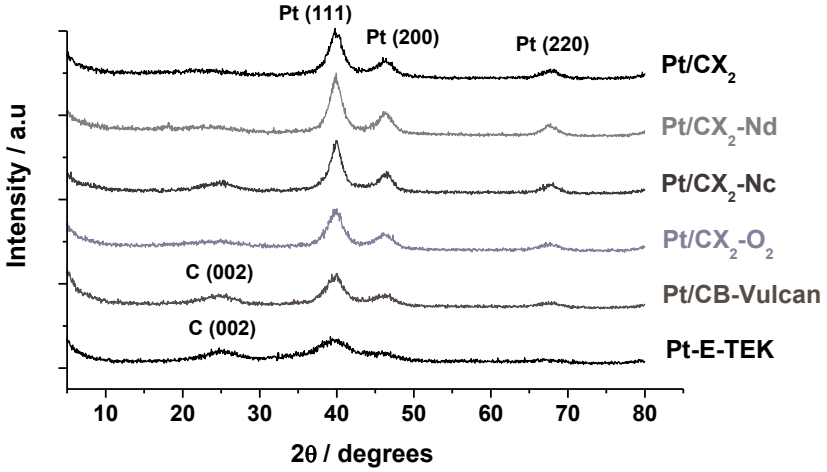
Pt (111)
Pt (200)
Pt (220)
Pt/CX2
Pt/CX2-Nd
Pt/CX2-Nc
Pt/CX2-O2
C (002)
Pt/CB-Vulcan
C (002)
Pt-E-TEK
Intensity / a.u
10
20
30
40
50
60
70
80
2θ / degrees

Figure 3.

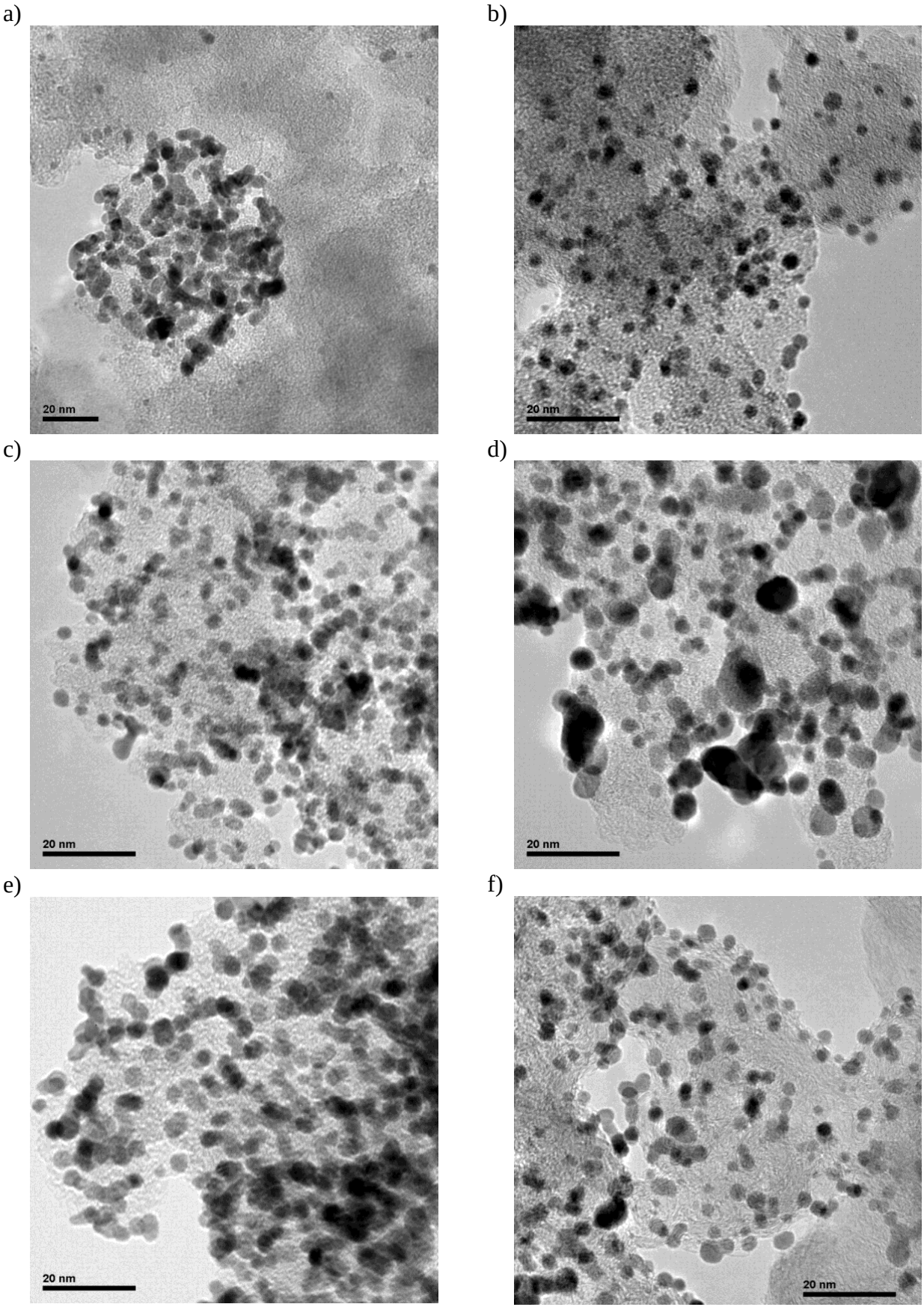

Figure 4.

a)

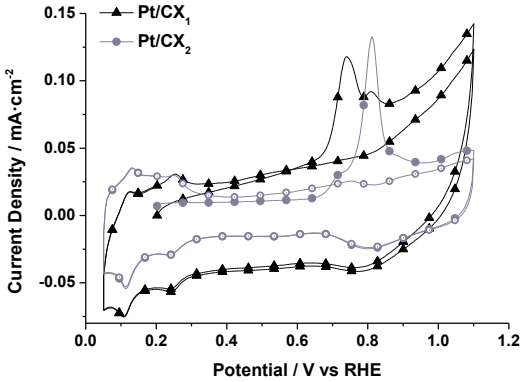

b)

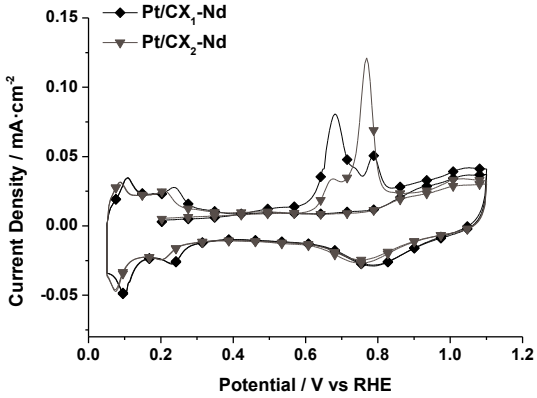

c)

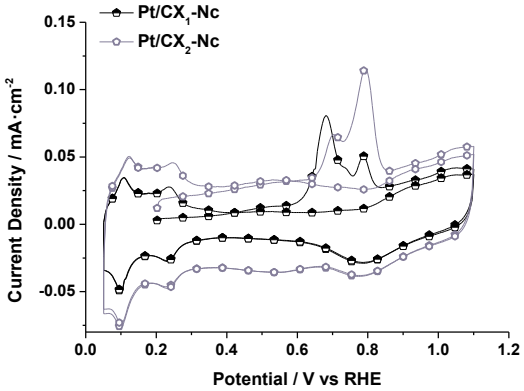

d)

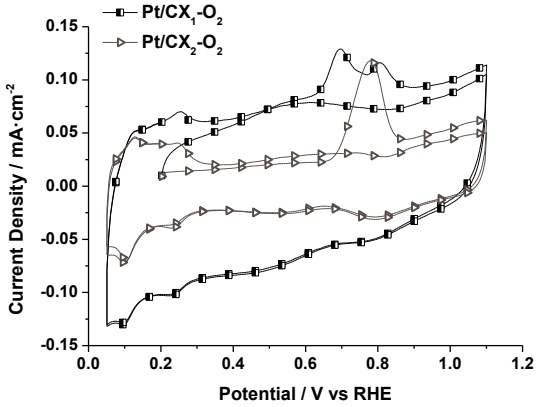

e)

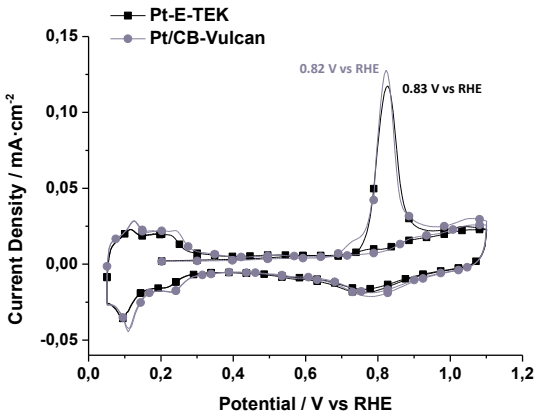

Figure 5.

a)

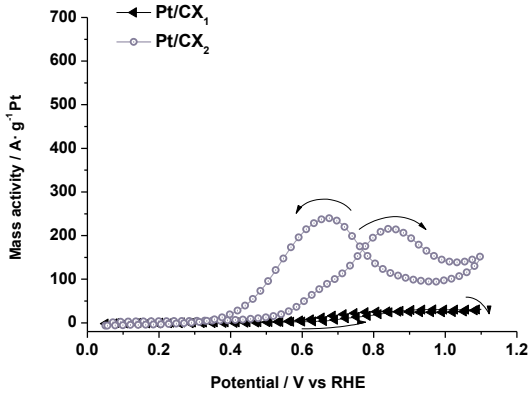

b)

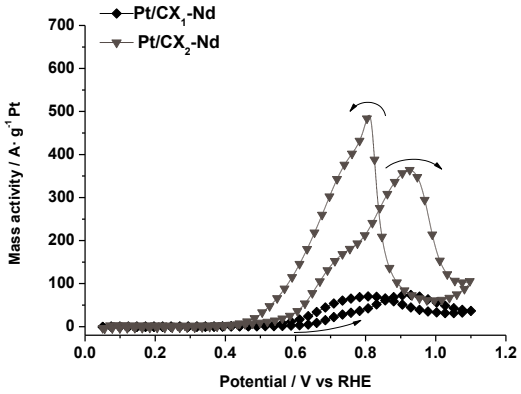

c)

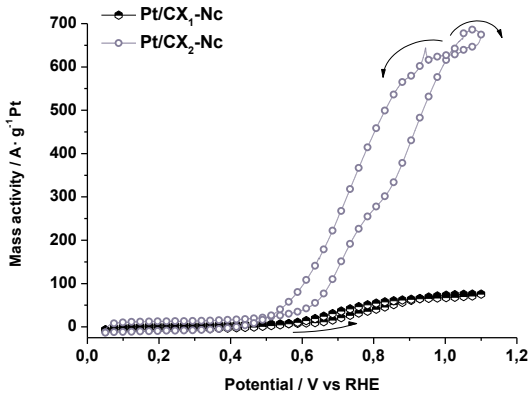

d)

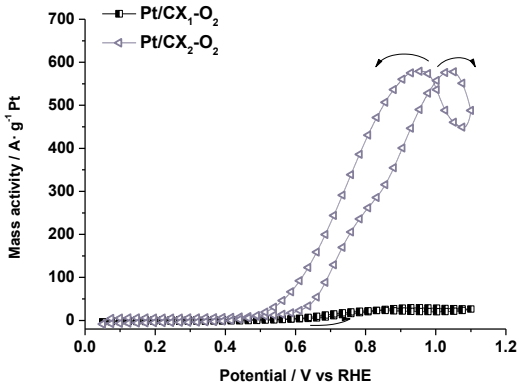

e)

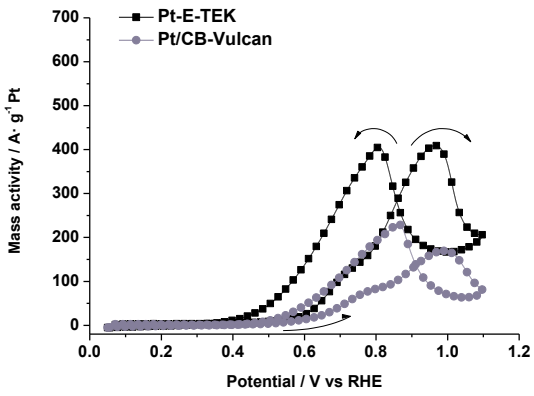

Figure 6.

a)

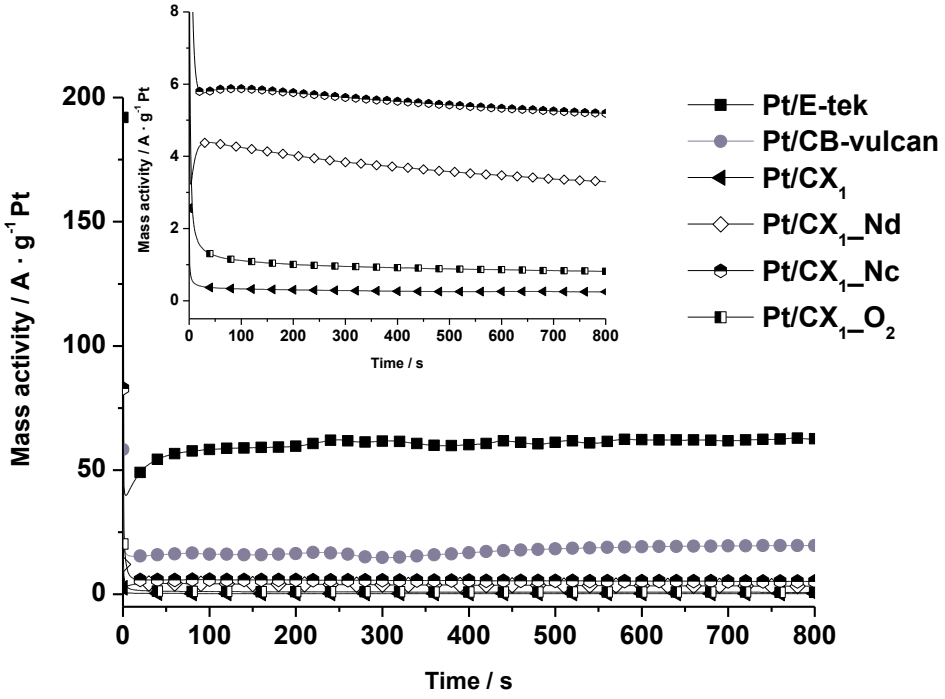
Mass activity / A · g-1 Pt
Time / s
Pt/E-tek
Pt/CB-vulcan
Pt/CX1
Pt/CX1_Nd
Pt/CX1_Nc
Pt/CX1_O2

b)

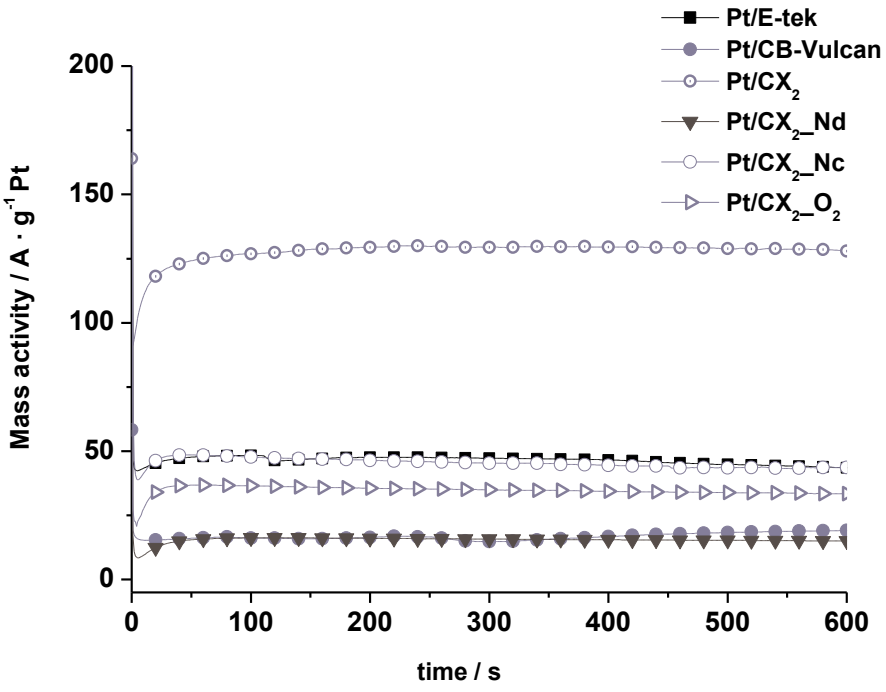
Mass activity / A · g-1 Pt
time / s
Pt/E-tek
Pt/CB-Vulcan
Pt/CX2
Pt/CX2_Nd
Pt/CX2_Nc
Pt/CX2_O2